Synsint Research Group

Available online at www.synsint.com

Synthesis and Sintering

ISSN 2564-0186 (Print), **ISSN** 2564-0194 (Online)

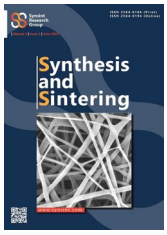

Research article

Mechanochemical synthesis of sulfur nanoparticles from industrial waste for enhanced Hg(II) adsorption

Leyla Karamzadeh [a,*], **Esmaeil Salahi** [a], **Iman Mobasherpour** [a], **Armin Rajabi** [b], **Masomeh Javaheri** [a]

[a] *Department of Ceramic, Materials and Energy Research Center, Karaj, Iran*
[b] *Institute of Sustainable Energy (ISE), Universiti Tenaga Nasional (UNITEN), Selangor, Malaysia*

A B S T R A C T

In this study, sulfur extracted from gas industry waste was utilized as an adsorbent for mercury ions (Hg^{2+}) in aqueous solutions. To enhance its adsorption capacity, a mechanical wet grinding process using a water–alcohol medium was employed to reduce particle size and increase surface area. Compared to dry grinding, the wet method significantly improved performance. BET analysis revealed an increase in specific surface area from 3.1 m^2/g (untreated sulfur) to 26.7 m^2/g after wet milling. BJH analysis showed the development of uniform micro- and mesopores in the 1–10 nm range, ideal for heavy metal adsorption. XRD and FTIR confirmed the preservation of sulfur's crystalline structure and the formation of S–S bonds, while SEM images revealed nanoparticles ranging from 30–100 nm. Batch adsorption experiments demonstrated an increase in mercury ion removal efficiency from 45% (raw sulfur) to 91% (wet-milled sulfur), and the adsorption capacity rose from 12 mg/g to 26 mg/g. These results confirm that wet grinding in a water–alcohol system is an effective strategy for enhancing the physicochemical properties and adsorption performance of sulfur for mercury remediation.

KEYWORDS

Nano-sulfur
Mercury
Adsorption
Waste
Mechanical milling

OPEN ACCESS

1. Introduction

Mercury is a toxic heavy metal that poses significant environmental and public health risks due to its persistence and bioaccumulation in aquatic ecosystems. It enters water bodies primarily through industrial effluents originating from sectors such as mining, electronics, and chemical manufacturing. Once in the environment, mercury can be transformed into more toxic forms, such as methylmercury, and rapidly bioaccumulates through the food chain, affecting aquatic life and human health by causing neurological, developmental, and carcinogenic effects [1, 2].

To mitigate mercury contamination, various treatment methods have been developed, including chemical precipitation, ion exchange, reverse osmosis, and chemical oxidation. However, these conventional approaches often face limitations such as high operational costs, generation of secondary waste, and incomplete removal of heavy metals [3, 4]. As a result, adsorption has emerged as a promising alternative due to its operational simplicity, cost-effectiveness, and potential for high removal efficiency [5–7].

Sulfur has attracted considerable attention as an effective adsorbent for mercury remediation due to its strong chemical affinity for mercury ions (Hg^{2+}). Its ability to readily bind with metal ions enables the efficient removal of mercury from aqueous solutions and other contaminated environments. It can form stable mercury-sulfur compounds, enabling the efficient separation of mercury from aqueous systems. It is abundant and can be sourced from industrial byproducts,

* Corresponding author. *E-mail address:* l.karamzadeh@merc.ac.ir (L. Karamzadeh)
Received 23 July 2024; Received in revised form 5 May 2025; Accepted 5 May 2025.

https://doi.org/10.53063/synsint.2025.52237

including waste from the gas industry, making it both a sustainable and cost-effective material [8–10].

To enhance its adsorption capacity, sulfur is often processed into nanoscale structures. Nanostructured sulfur offers a higher surface area and more active sites for mercury binding. Among various methods, mechanical milling —a top-down method— has been employed for the production of sulfur nanoparticles. This approach not only reduces particle size but also activates the surface of the material, improving its adsorption properties. The addition of activating solvents such as water or alcohol during milling further increases surface reactivity [11–14].

Nanomaterials are typically synthesized using two main approaches: top-down and bottom-up methods. In the top-down approach, bulk materials are broken down into fine or nanoscale particles through physical processes such as mechanical milling, lithography, or abrasion.

Recent studies have also explored the combination of sulfur with other materials, such as activated carbon and metal nanoparticles, to further enhance mercury adsorption performance through synergistic effects [14–18].

Overall, the development of sulfur-based nanomaterials offers a promising and sustainable strategy for the efficient removal of mercury from contaminated water systems [19].

2. Experiments

2.1. Material and method

Sulfur nanoparticles were produced through mechanical milling, a top-down technique widely used for nanomaterial fabrication. This method is one of the most common mechanical approaches for generating sulfur-based nanomaterials.

In this study, sulfur was recovered from gas industry waste and processed into nanoparticles using a planetary ball mill. To prepare the slurry for milling, the sulfur powder was mixed with distilled water in a 1:3 weight ratio (sulfur: water). The slurry was placed into a milling chamber containing alumina balls of five different diameters (2–12 mm), occupying one-third of the chamber volume. Milling was carried out at 300 rpm for 12 h. The ball-to-powder mass ratio was maintained at 10:1 to ensure optimal grinding efficiency, as supported by previous studies.

Table 1 summarizes the key specifications of the planetary ball mill used in this study, along with additional parameters essential for reproducibility.

Table 1. Specifications of the planetary ball mill.

Specification	Description
Control system	Adjustable time and speed
Final powder particle size	Down to the nanometer scale
Powder protection during milling	Capable of vacuum or inert gas protection
Ball-to-powder ratio	10:1
Ball material	Alumina
Chamber material	Stainless steel
Milling environment	Ambient air (no vacuum or inert gas applied)

The adsorption of mercury ions using sulfur nanoparticles was subsequently investigated under controlled laboratory conditions. For this purpose, an aqueous solution of high-purity mercury(II) chloride ($HgCl_2$, Merck, Germany) was prepared by dissolving the compound in distilled water to achieve an initial Hg^{2+} concentration of 75 mg/l. For each experiment, 500 ml of the mercury solution was mixed with 0.5 g of sulfur nanoparticles in a glass beaker and stirred at a constant speed of 300 rpm. The temperature was maintained at 25 ± 2 °C, and the pH of the solution was adjusted to 6.5. Mixing was carried out in a clean glass beaker using a magnetic stirrer under these controlled conditions. At predetermined time intervals (5, 10, 30, and 60 min), small aliquots were withdrawn using a pipette, centrifuged at 3000 rpm, and the supernatant was analyzed to determine the residual mercury ion concentration.

The adsorption capacity was calculated based on the difference in mercury concentration before and after treatment. Mercury concentrations were determined using an atomic absorption spectrophotometer (GBC932 Plus), and each measurement was performed in duplicate to ensure accuracy.

Following the adsorption process, the solids were separated by centrifugation at 3000 rpm for 10 min, air-dried at room temperature, and preserved for subsequent characterization. In subsequent tests, variables such as adsorbent dosage, contact time, and adsorbent type were systematically varied to evaluate their effects on adsorption efficiency. Additionally, the masses of both adsorbate and adsorbent were varied in later experiments.

As part of the continuation of this study, the structure of sulfur obtained from gas industry waste was analyzed to gain insights into the mercury adsorption mechanisms. Unlike the more commonly used dry milling methods, a wet ball milling approach was adopted using sulfur and water.

The wet milling approach resulted in reduced particle size and enhanced mesoporosity compared to dry milling. These structural improvements were confirmed by BET surface area analysis and particle size measurements, which demonstrated an increased surface area and a decreased average particle size (as presented in the next section). This modification positively influenced the contact surface area, while the enhanced mesoporous structure significantly contributed to the increased mercury adsorption capacity of the sulfur nanoparticles. All procedures were conducted following methodologies adapted from previous studies [3–5].

2.2. Characterization

The raw and wet-milled sulfur samples were characterized using several analytical techniques to assess their structural, chemical, and morphological properties. X-ray diffraction (XRD) was used to determine crystallinity and phase composition, while Fourier-transform infrared spectroscopy (FTIR) provided information on chemical bonding and functional groups. Scanning electron microscopy (SEM) examined particle morphology and size distribution. Additionally, nitrogen adsorption–desorption analysis (BET and BJH) evaluated specific surface area and pore size distribution. These characterization methods together helped to elucidate the key physical and chemical features that influence mercury adsorption efficiency.

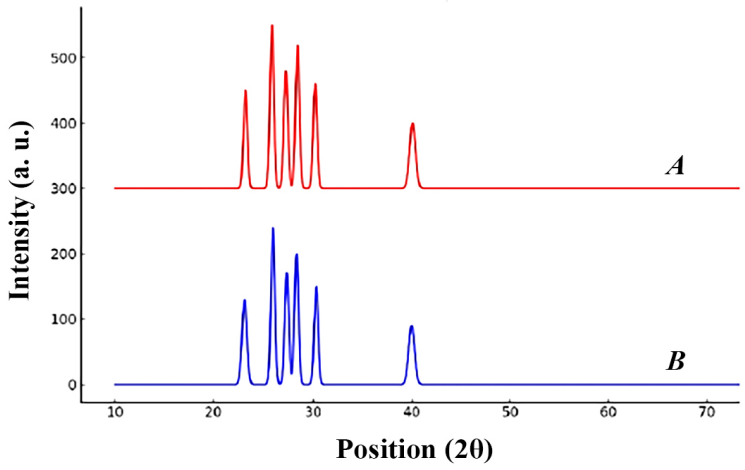

Fig. 1. X-ray diffraction (XRD) patterns (A: the raw sulfur sample and B: the mechanically processed sulfur sample).

3. Results and discussion

X-ray diffraction (XRD) analysis was performed to investigate the crystallographic structure and phase composition of sulfur samples before and after mechanical processing. The results of the XRD analysis are presented in Fig. 1. Peaks observed at approximately 23 °, 25.8 °, and 27.6 ° correspond to standard card number 9011362. The characteristic peaks of elemental sulfur (S_8) appeared at 23.6 °, 27.6 °, and 27.8 °, corresponding to the (222), (206), and (026) crystal planes, respectively.

Additional peaks indicate the presence of metastable or unstable sulfur phases. The similarity in peak positions before and after mechanical processing suggests that no significant impurities were introduced during the milling process. However, the XRD pattern of the wet-milled sample shows broader peaks, indicating a reduced crystallite size and nanocrystalline nature. The estimated average crystallite size of the processed sample was approximately 28 nm, compared to 95 nm for the raw sample. These results confirm that the wet ball milling process effectively reduces particle size while preserving the original crystalline structure of sulfur.

Maintaining high crystallinity and chemical purity after processing can significantly enhance the surface-related properties of sulfur, especially for adsorption-based applications such as mercury removal. These results highlight the potential of wet mechanical processing in producing nanostructured sulfur adsorbents from industrial waste, supporting both resource recovery and environmental remediation.

The FTIR spectrum of the processed sulfur sample is demonstrated in Fig. 2. This spectrum displays a characteristic absorption band around 462 cm^{-1}, corresponding to S–S stretching vibrations. No significant absorption bands were observed in the 1000–4000 cm^{-1} range, indicating the absence of oxygen- or hydrocarbon-based functional groups. These findings confirm that the chemical purity of sulfur was maintained after wet milling. However, future studies are recommended to include extended FTIR scans to identify any weak or surface-related functional groups potentially influencing adsorption mechanisms.

Fig. 3 shows the SEM images of the processed sulfur sample. The sulfur particles exhibit an amorphous-like microstructure with relatively uniform distribution at the nanoscale. While some particles appear spherical or polyhedral in shape, thin, irregularly shaped sulfur sheets were also observed, consistent with typical nanostructured sulfur morphologies. These observations confirm that mechanical processing effectively reduces particle size. Further quantitative analysis—such as image-based particle size estimation or dynamic light scattering (DLS)—is recommended to obtain more precise data. In addition, presenting a comparative summary of crystallite size (from XRD), particle size (from SEM or DLS), and specific surface area (from BET) in future work could provide a more comprehensive understanding of the material's structure–property relationships.

The specific surface area and pore structure of sulfur samples before and after processing were evaluated using Brunauer–Emmett–Teller (BET) and Barrett–Joyner–Halenda (BJH) analyses. Fig. 4a shows the BJH adsorption isotherm of the raw sulfur sample, which displays a broad and poorly defined pore size distribution between 15 and 100 nm, with a dominant peak around 50 nm. These macropores are typically inefficient for the adsorption of heavy metal ions due to their limited surface interaction. In contrast, the processed sulfur sample (Fig. 4b) exhibits a significantly narrower and more uniform distribution of micropores (1–5 nm) and mesopores (5–10 nm), with distinct peaks around 2 nm and 9 nm. This improvement in pore structure indicates that wet mechanical processing effectively enhances porosity and increases the surface area of sulfur. Notably, previous studies have reported that pores in the 1–10 nm range are optimal for adsorption and catalytic processes [20], which supports the observed improvement in mercury adsorption performance of the processed sample.

To enhance data clarity and interpretability, the isotherms should include explicit axis labels, such as pore diameter (nm) and dV/dlog (D) for pore volume. It should also be clearly stated whether the curves represent the adsorption or desorption branches of the isotherm. Moreover, including a summary table comparing crystallite size (from XRD) and specific surface area (from BET) for both raw and processed samples would provide a more comprehensive comparison of structural changes resulting from mechanical processing.

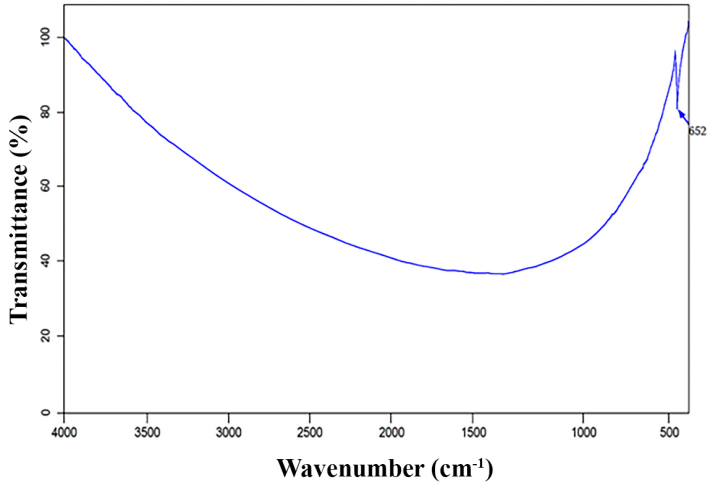

Fig. 2. Fourier-transform infrared (FTIR) spectrum of the mechanically processed sulfur.

Furthermore, while the improved pore characteristics qualitatively support the claim that sulfur processing enhances adsorption efficiency, this argument could be further strengthened by benchmarking against other sulfur-based or waste-derived adsorbents reported in the literature. A comparative table summarizing adsorption capacities (e.g., mg/g for Hg^{2+}), pore size distributions, and BET surface areas across various materials would provide valuable context and help substantiate the improved performance of the current system.

In the investigation of mercury adsorption using sulfur-based adsorbents, two key performance indicators were evaluated. The first is the adsorption capacity per unit mass of adsorbent (q, mg/g), which is defined by Eq. 1 [21]:

$$q = (C_i - C_f) \times V/m \quad (1)$$

where q is the mercury ions adsorption capacity, C_i and C_f are the initial and final concentrations of Hg^{2+} ions (mg/l), respectively; V is the volume of the solution (l), and m is the mass of the adsorbent used (g). The second performance indicator is the removal efficiency (%) of mercury ions, which is defined by Eq. 2 [21]:

$$\text{Removal efficiency} = ((C_i - C_f)/Ci) \times 100 \quad (2)$$

These parameters were evaluated for two sulfur-based samples—dry-milled (S-dry) and wet-milled (S-wet)—to assess the influence of particle morphology and surface area on mercury adsorption performance.

Table 2 shows a comparison between dry-milled (S-dry) and wet-milled (S-wet) sulfur samples in terms of surface area, average pore size, and mercury adsorption performance. As can be seen in the table, the BET surface area of the S-wet sample (32.5 m^2/g) is significantly higher than that of the S-dry sample (14.3 m^2/g), and the pore size also changed from predominantly macroporous (about 50 nm) in the dry sample to micro- and mesoporous (1–10 nm) in the wet-milled sample. This improvement in surface properties seems to have a direct effect on mercury adsorption. The adsorption capacity increased from 12 mg/g

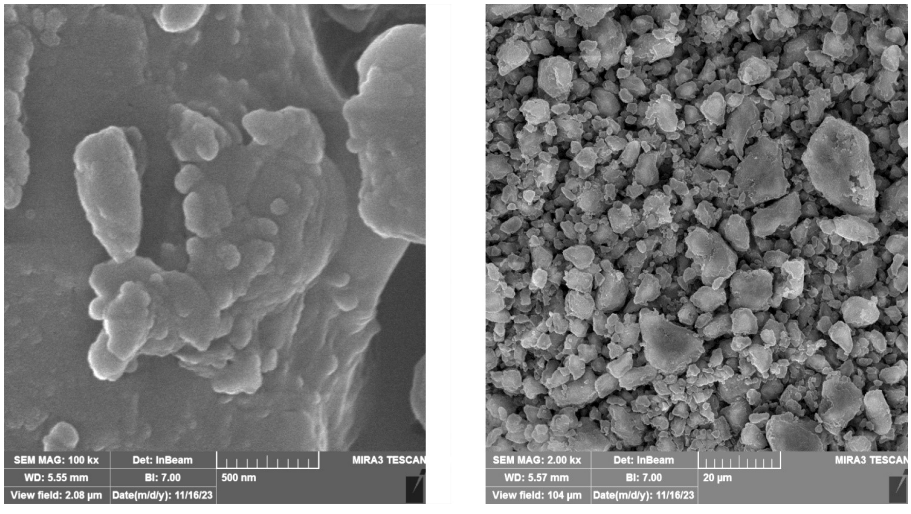

Fig. 3. SEM images of the processed sulfur nanoparticles at two different magnifications.

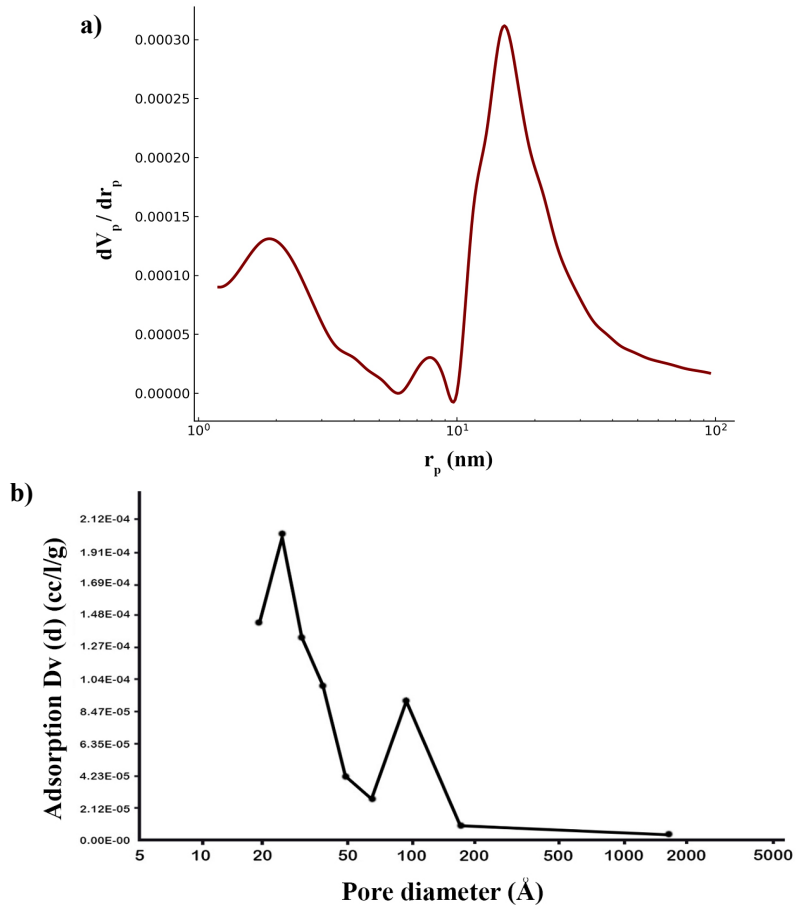

Fig. 4. BJH pore size distribution curves for a) raw sulfur and b) sulfur sample after wet ball milling.

for S-dry to 26 mg/g for S-wet, and the removal efficiency also improved from 8% to 17.3%. These results indicate that wet milling has a significant effect on enhancing the performance of sulfur as a mercury adsorbent.

Fig. 5 (a, b, and c) shows the kinetics and efficiency of mercury removal for both sulfur samples tested under the same conditions (initial Hg^{2+} concentration = 75 mg/l, adsorbent dosage = 0.5 g/l, and contact time = 60 minutes). A large portion of mercury uptake occurred in the first 5 minutes for both S-wet and S-dry, suggesting a rapid initial adsorption process. However, after reaching equilibrium, S-wet showed a much higher adsorption capacity (26 mg/g) than S-dry (12 mg/g), and the removal efficiency also increased from 8% to 17.3%. This difference can be mainly attributed to the improved pore structure, smaller crystallite size, and higher surface area of the S-wet sample.

The adsorption of Hg^{2+} by sulfur is generally understood to involve a combination of surface complexation, chemisorption, and potentially precipitation, depending on the structural form and surface chemistry of the material. Although the dominant mechanism remains unclear, the enhanced performance of S-wet is consistent with literature reports that highlight the role of surface defects and amorphous regions in facilitating ion diffusion and interaction.

Mechanistically, increased particle size reduces the surface-to-volume ratio, limiting the availability of active adsorption sites. High crystallinity also limits ion diffusion due to fewer structural defects and less permeable lattice structures. Conversely, low-crystalline or amorphous sulfur structures exhibit enhanced solubility and defect-rich surfaces that facilitate mercury ion adsorption with lower energy requirements.

Table 2. ET area, pore size, and Hg^{2+} uptake for S-dry vs. S-wet (75 mg/l Hg^{2+}, 0.5 g/ l, 60 min).

Sample	BET surface area (m^2/g)	Average pore diameter (nm)	Hg^{2+} adsorption capacity (mg/g)	Removal efficiency (%)
S-dry	14.3	~50 (macroporous)	12	8
S-wet	32.5	1–10 (micro/mesoporous)	26	17.3

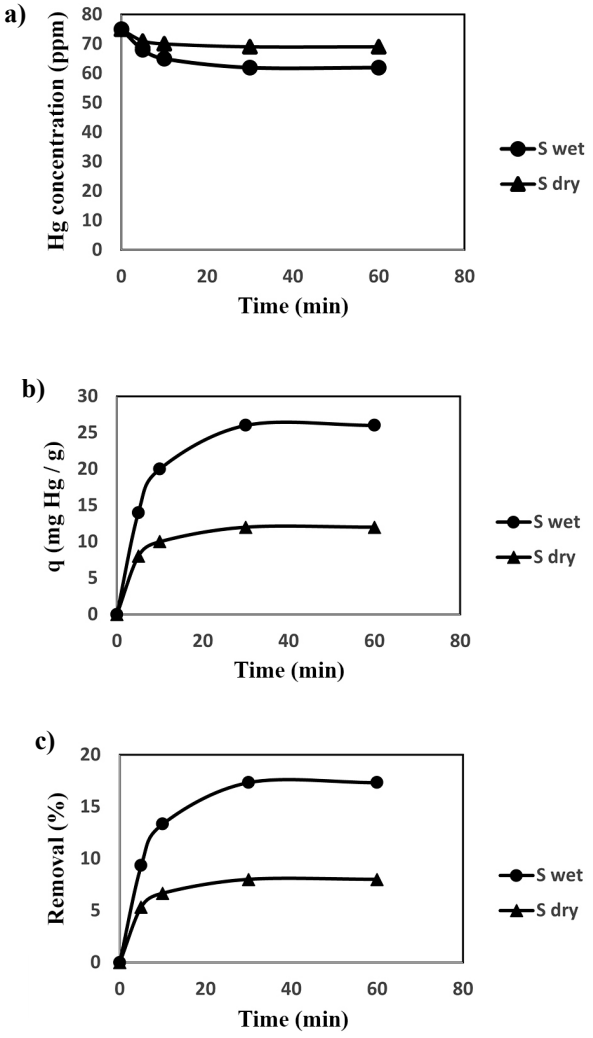

Fig. 5. kinetics and efficiency of mercury removal for both sulfur samples (initial Hg^{2+} concentration = 75 mg/l, adsorbent dosage = 0.5 g/l, and contact time = 60 minutes).

Comparison of BET surface area, average pore diameter, and Hg^{2+} adsorption performance between dry-milled (S-dry) and wet-milled (S-wet) sulfur samples under initial conditions of 75 mg/l Hg^{2+} concentration, 0.5 g/l adsorbent dosage, and 60 minutes equilibrium time:

- **Average pore diameter:** S-dry retains large macropores (~50 nm), while S-wet exhibits narrow micro- and mesopores (1–10 nm).
- **Adsorption capacity & removal efficiency:** measured at 75 mg/l Hg^{2+}, 0.5 g/l adsorbent dosage, and 60 min equilibrium time.

4. Conclusions

This work demonstrates for the first time that sulfur nanoparticles derived from gas industry waste via wet ball milling exhibit markedly enhanced mercury adsorption performance compared to raw sulfur. The wet-milled material achieved a BET surface area of 26.7 m^2/g—an 8.6-fold increase over raw sulfur—and removed Hg^{2+} at 26 mg/g, more than double the 12 mg/g capacity of unmilled sulfur. The combination of uniform micropores (1–5 nm) and mesopores (5–10 nm), with a defect-rich, low crystallinity structure, underlies this improvement, providing abundant active sites and reduced diffusion barriers. By converting an industrial byproduct into a high-performance adsorbent, this approach offers a cost-effective, sustainable route for mercury remediation in wastewater treatment plants. The scalability of wet ball milling suggests practical industrial deployment, turning waste sulfur into value-added nanomaterials. While batch tests confirm rapid kinetics and high capacity, continuous flow studies are needed to assess real-world performance. Further work should also explore the regeneration and reuse of sulfur adsorbents, long-term stability under variable water chemistries, and techno-economic analysis for large-scale implementation.

CRediT authorship contribution statement

Leyla Karamzadeh: Investigation, Methodology, Writing – original draft.
Esmaeil Salahi: Conceptualization, Supervision, Writing – review & editing.
Iman Mobasherpour: Funding acquisition, Validation.
Armin Rajabi: Data curation, Writing – review & editing.
Masomeh Javaheri: Supervision, Writing – review & editing.

Data availability

The data underlying this article will be shared on reasonable request to the corresponding author.

Declaration of competing interest

The authors declare no competing interests.

Funding and acknowledgment

This paper is derived from the PhD thesis of the first author. The authors would like to express their gratitude to the Materials and Energy Research Center for their support of this research work under grant number 381399055.

References

[1] M. Razali, Y.Q. Zhao, M. Bruen, Effectiveness of a drinking-water treatment sludge in removing different phosphorus species from aqueous solution, Sep. Purif. Technol. 55 (2007) 300–306. https://doi.org/10.1016/j.seppur.2006.08.010.
[2] C.S. Silva, R.T. Oliveira, Methylmercury concentrations in fish from the lower Paraíba do Sul river, southeastern Brazil, Chemosphere. 202 (2018) 483–490. https://doi.org/10.1016/j.chemosphere.2018.03.156.
[3] O. Rodríguez, I. Padilla, H. Tayibi, A. López-Delgado, Concerns on liquid mercury and mercury-containing wastes: A review of the treatment technologies for the safe storage, J. Environ. Manage. 113 (2012) 10–25. https://doi.org/10.1016/j.jenvman.2012.07.028.
[4] H. Mason, P. Hindell, N. Williams, Biological monitoring and exposure to mercury, Occup. Med. (Lond.). 51 (2001) 2–11. https://doi.org/10.1093/occmed/51.1.2.
[5] S. Kales, R. Goldman, Mercury exposure: current concepts, controversies, and clinical experience, J. Occup. Environ. Med. 44 (2002) 143–154.
[6] M.J. Amiri, J. Abedi-Koupai, S. Eslamian, M. Arshadi, Adsorption of Pb(II) and Hg(II) ions from aqueous single-metal solutions by using surfactant-modified ostrich bone waste, Desal. Water Treat. 53 (2015) 1–18. https://doi.org/10.1080/19443994.2014.940441.
[7] R. Foroutan, S.J. Peighambardoust, A. Ahmadi, A. Akbari, S. Farjadfard, B. Ramavandi, Adsorption of mercury, cobalt, and nickel with a reclaimable and magnetic composite of hydroxyapatite/Fe3O4/polydopamine, J. Environ. Chem. Eng. 9 (2021) 105709. https://doi.org/10.1016/j.jece.2020.105709.
[8] M. Naushad, T. Ahamad, Z.A. AlOthman, A.H. Al-Muhtaseb, Green and eco-friendly nanocomposite for the removal of toxic Hg(II) metal ion from aqueous environment: adsorption kinetics and isotherm modelling, J. Mol. Liq. 279 (2019) 1–8. https://doi.org/10.1016/j.molliq.2019.01.134.
[9] R. Sun, X. Li, Y. Zhang, Theoretical research on reaction of solid sulfur allotropes with elemental mercury, Chem. Eng. J. 407 (2021) 127113. https://doi.org/10.1016/j.cej.2020.127113.
[10] S.J. Rettig, J. Trotter, Refinement of the structure of orthorhombic sulfur, α-S8, Acta Crystallogr. C. 43 (1987) 2260–2262. https://doi.org/10.1107/S0108270187088152.
[11] Y.H. Yeom, S.H. Song, Y. Kim, The crystal structure of a sulfur sorption complex of the dehydrated partially Co2+-exchanged zeolite A, Bull. Korean Chem. Soc. 16 (1995) 823–826. https://doi.org/10.5012/bkcs.1995.16.9.823.
[12] A.K. Deb Singha, N. Dhume, K. Dasgupta, S.M. Ali, K.T. Shenoy, S. Mohan, Sulphur ligand functionalized carbon nanotubes for removal of mercury from wastewater – experimental and density functional theoretical study, Sep. Sci. Technol. 54 (2019) 1573–1587. https://doi.org/10.1080/01496395.2018.1529044.
[13] T. Velempini, K. Pillay, Sulphur functionalized materials for Hg(II) adsorption: A review, J. Environ. Chem. Eng. 7 5 (2019) 10335. https://doi.org/10.1016/j.jece.2019.103354.
[14] J. Wang, B. Deng, X. Wang, J. Zheng, Adsorption of aqueous Hg(II) by sulfur-impregnated activated carbon, Environ. Eng. Sci. 26 (2009) 1092–8758. https://doi.org/10.1089/ees.2008.0418.
[15] Y. Ting, X. Chen, L. Zhou, Using raw and sulfur-impregnated activated carbon as active cap for leaching inhibition of mercury and methylmercury from contaminated sediment, J. Hazard. Mater. 354 (2018) 116–124. https://doi.org/10.1016/j.jhazmat.2018.02.053.
[16] B. Zhang, L. Li, H. Zhao, Magnetic sulfur-doped carbons for mercury adsorption, J. Colloid Interface Sci. 603 (2021) 728–737. https://doi.org/10.1016/j.jcis.2021.04.051.
[17] A. Kumar, H.-W. Song, S. Mishra, W. Zhang, Y.-L. Zhang, Application of microbial-induced carbonate precipitation (MICP) techniques to remove heavy metal in the natural environment: A critical review, Chemosphere. 318 (2023) 137894. https://doi.org/10.1016/j.chemosphere.2023.137894.
[18] B. Karwowska, E. Sperczyńska, Organic matter and heavy metal ions removal from surface water in processes of oxidation with ozone, UV irradiation, coagulation and adsorption, Water. 14 (2022) 3763. https://doi.org/10.3390/w14223763.
[19] U.Y. Qazi, A. Ikhlaq, A. Akram, O.S. Rizvi, F. Javed, Novel vertical flow wetland filtration combined with Co-zeotype material based catalytic ozonation process for the treatment of municipal wastewater, Water. 14 (2022) 3361. https://doi.org/10.3390/w14213361.
[20] M. Noman, M. Shahid, T. Ahmed, M.B.K. Niazi, S. Hussain, Use of biogenic copper nanoparticles synthesized from a native Escherichia sp. as photocatalysts for azo dye degradation and treatment of textile effluents, Environ. Pollut. 257 (2020) 113514. https://doi.org/10.1016/j.envpol.2019.113514.
[21] L.F. Muhaisen, F.F. Muhaisen, Z.M. Abdulkareem, Removal of cadmium ions from aqueous solution by batch experiment, Iraqi J. Chem. Petrol. Eng. 17 (2016) 101–108. https://doi.org/10.31699/IJCPE.2016.3.9.